SUPPORTING INFORMATION

Strong Circularly Polarized Electroluminescence based on Chiral Salen-Zn(II) Complex Monomer Chromophore

Yihan Chen,[a] Xiaojing Li,[b] Nengquan Li,[c] Yiwu Quan*[c], Yixiang Cheng*[b] and Yanfeng Tang*[a]

[a] School of Chemistry and Chemical Engineering, Nantong University, Nantong 226019,China
E-mail: tangyf@ntu.edu.cn

[b] Key Lab of Mesoscopic Chemistry of MOE and Jiangsu Key Laboratory of Advanced Organic Materials, School of Chemistry and Chemical Engineering, Nanjing University, Nanjing 210023, China
E-mail: yxcheng@nju.edu.cn

[c] key Laboratory of High Performance Polymer Material and Technology of Ministry of Education, Department of Polymer Science and Engineering, School of Chemistry and Chemical Engineering, Nanjing University, Nanjing 210023, China.
E-mail: quanyiwu@nju.edu.cn

Contents:

SI 1. Instrumentation and Measurements

All starting materials were purchased from Acros, Alfa Aesar, Energy and used directly. Thermogravimetric analysis (TGA) was performed on a Pyris 1 TGA Instrument (PerkinElmer, America). The thermal stability of the sample was determined by measuring the weight loss at a heating rate of 10 °C/min from 30 to 690 °C under a nitrogen atmosphere. Absorption and PL spectra of the blends at various blending ratios were measured by a Cary 300 UV–*vis* spectrometer (Agilent Technologies) and a FluoroMax-3 (Horiba Jobin Yvon), respectively. The thin film of ZnL complexes were deposited under a vacuum of 8×10^{-5} Pa at a deposition rate of 1~2 Å/s, and the thickness of the resulting thin films were measured to be around 100 nm, as measured by a Dektak surface profilometer. The thin film samples were used for the measurements of CD, UV-*vis*, PL and CPL spectra at room temperature.

SI 2. Synthesis procedures of the Chiral Salen-Zn(II) Complex (*R-/S*-ZnL)

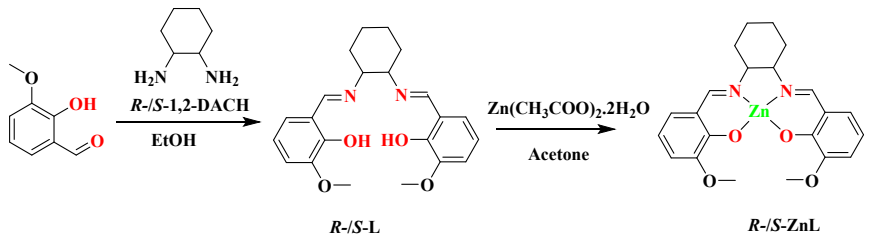

Scheme S1. The synthetic route to *R-/S*-ZnL enantiomers.

Synthesis.

***R-/S*-L** 3-Methoxysalicylaldehyde (2.0 g, 13.15 mmol) in ethanol (30 mL) was first treated with 1,2-diaminocyclohexane (0.75 g, 6.575 mmol) and the mixture was stirred for 12 h at room temperature. After cooling to room temperature, the mixture was put in the refrigerator for 24 hours to give needle-shaped yellow crystals. Yield: 2.2g, (88%) ^{1}H NMR (400 MHz, $CDCl_3$) δ 13.83 (s, 2H), 8.25 (s, 2H), 6.88 – 6.83 (m, 2H), 6.80 (d, J = 7.3 Hz, 2H), 6.72 (t, J = 7.8 Hz, 2H), 3.86 (s, 6H), 3.41 – 3.27 (m, 2H),1.91 (dd, J = 26.3, 11.8 Hz, 4H), 1.72 (dd, J = 21.4, 11.0 Hz, 2H), 1.57 – 1.38 (m, 2H). ^{13}C NMR (100 MHz, $CDCl_3$) δ 164.75, 151.56, 148.23, 123.15, 118.37, 117.88, 113.79, 72.41, 56.01, 33.02, 24.05.

***R-/S*-ZnL:** *R/S*-L (2.0g,5.233mmol) was added to the solution of acetone (15ml) and stirred to dissolve. Then $Zn(OAc)_2\cdot2H_2O$ (1.15 g, 6.575 mmol) was added to the mixture. The mixture was stirred at room temperature overnight, and the resulting yellow precipitation was collected by filtration and washed with acetone and ether. Yield: 2.13 g (92%) ^{1}H NMR (400 MHz, DMSO-d6) δ 8.32 (s, 2H), 6.84 (dd, J = 8.0, 1.6 Hz, 2H), 6.77 (dd, J = 7.6, 1.5 Hz, 2H), 6.35 (t, J = 7.7 Hz, 2H), 3.72 (s, 6H), 3.19 (d, J = 6.5 Hz, 2H), 2.44 (d, J = 9.8 Hz, 2H), 1.91 (d, J = 6.3 Hz, 2H), 1.54 – 1.26 (m, 4H). ^{13}C NMR (101 MHz, DMSO-d6) δ 165.10, 162.38, 152.85, 127.32, 119.00, 113.44, 111.34,

64.98, 55.56, 28.22, 24.33.

SI 3. NMR spectra

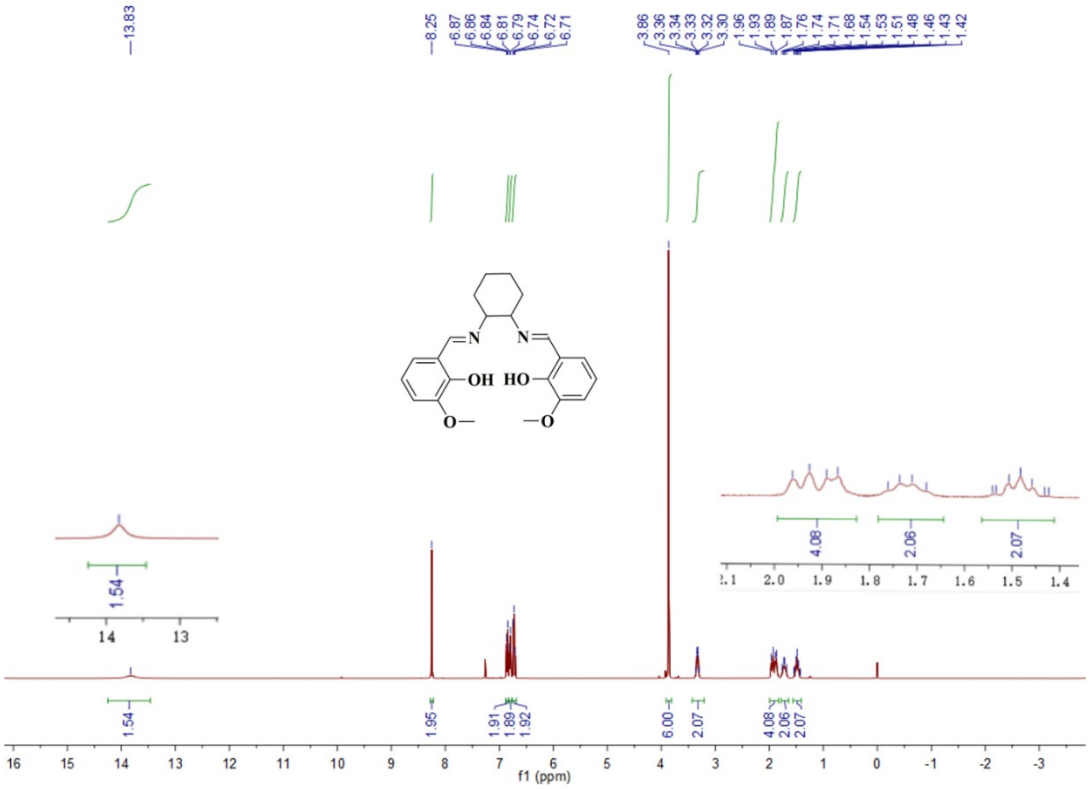

Figure S1. ^{1}H NMR of *R*-/*S*-L (400 MHz, $CDCl_3$).

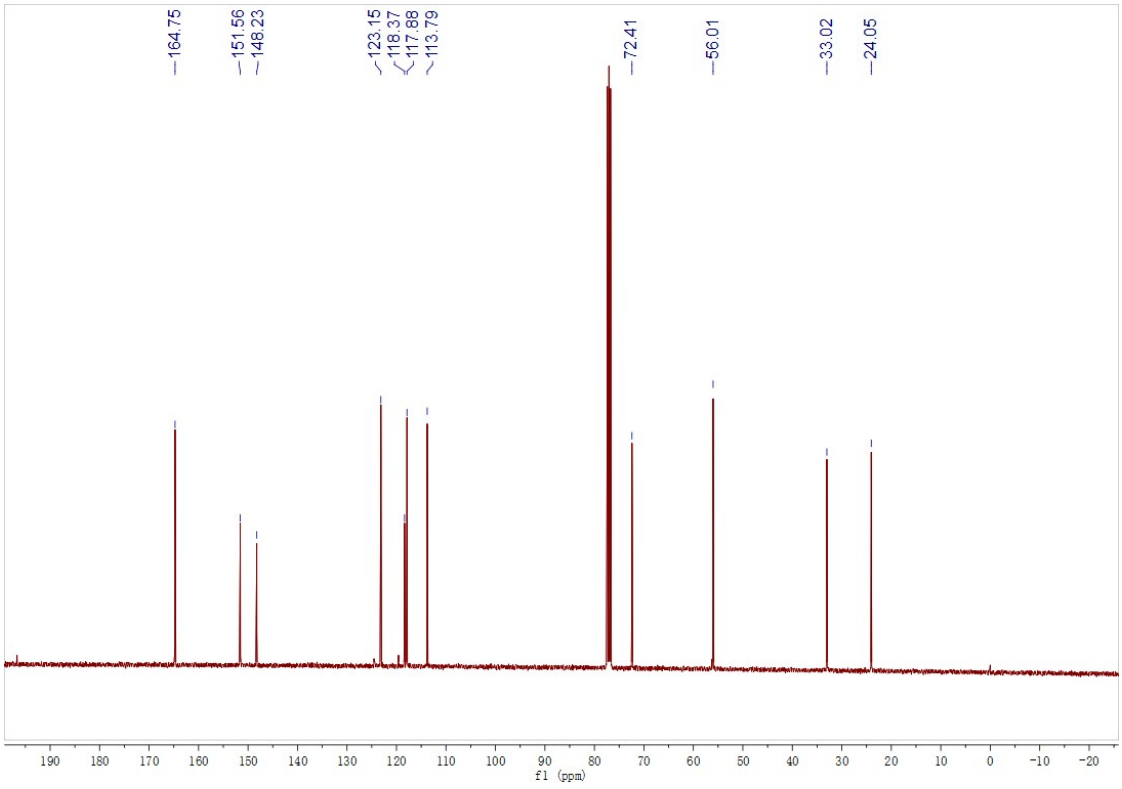

Figure S2. ^{13}C NMR of *R*-/*S*-L (400 MHz, $CDCl_3$).

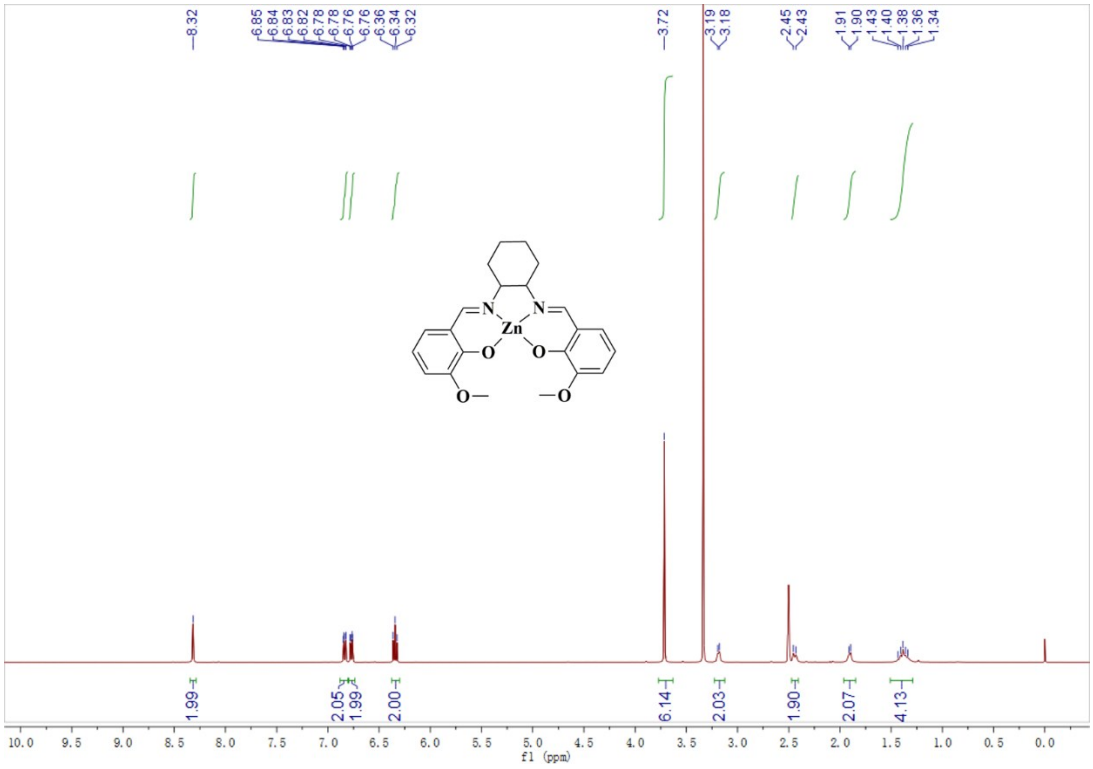

Figure S3. [1]H NMR of *R-/S*-ZnL (400 MHz, DMSO-d6).

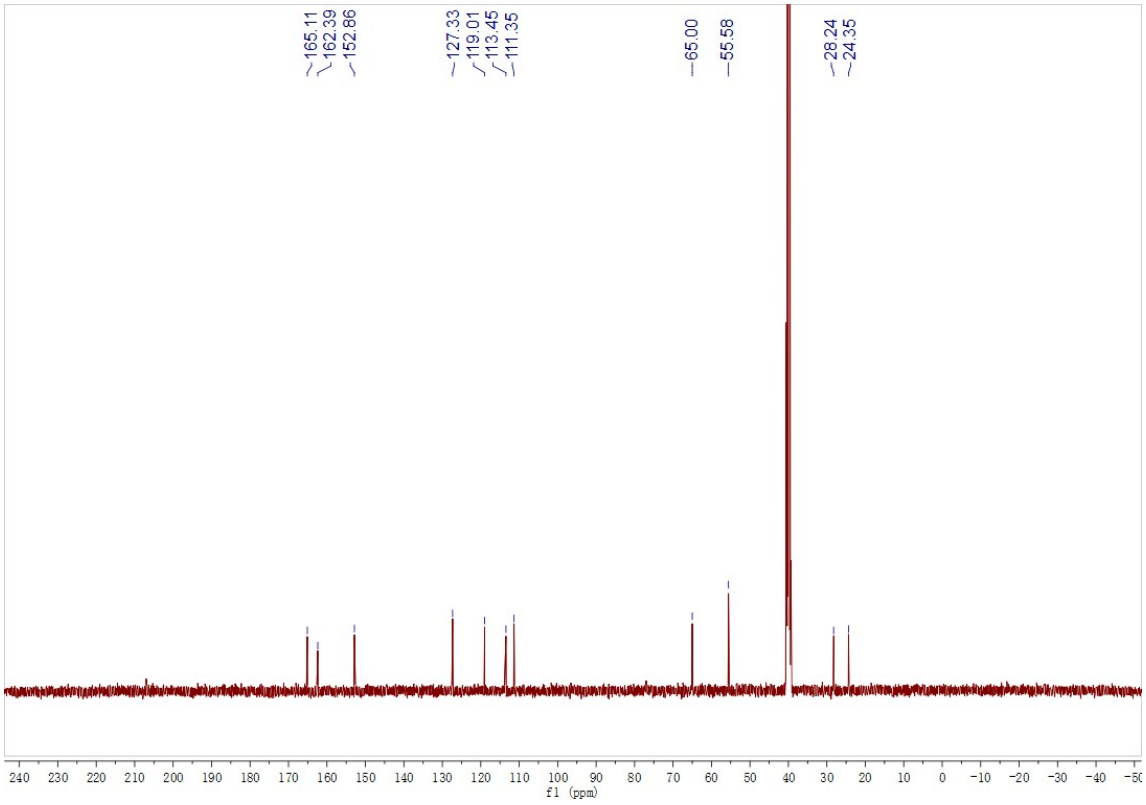

Figure S4. [13]C NMR of *R-/S*-ZnL (400 MHz, DMSO-d6).

SI 4. CD spectra of *R-/S*-ZnL in solution of THF and in KBr pellet-dispersed state

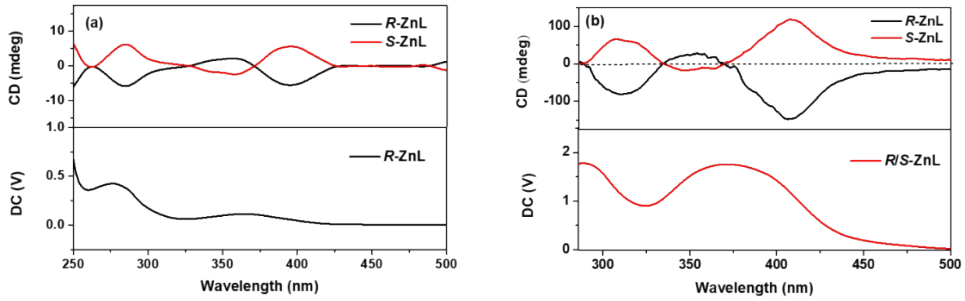

Figure S5. a) *R-/S*-ZnL in THF solution (1.0×10^{-5} mol·L^{-1}); b) CD spectra of *R-/S*-ZnL (1wt%) in KBr pellet-dispersed state.

SI 5. Thermo gravimetric analysis

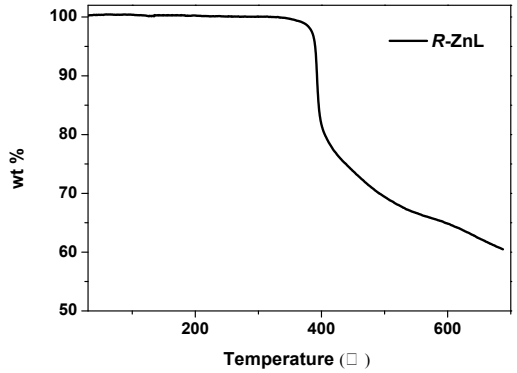

Figure S6. TGA of *R*-ZnL at a heating rate of 10 °C min^{-1}.

SI 6. Cyclic voltammogram analysis

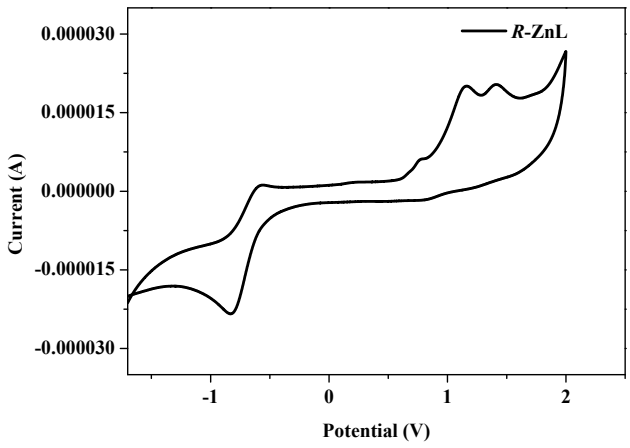

Figure S7. Cyclic voltammogram of the representative complex (*R*-ZnL) in 0.1 M *n*-Bu_4NBF_4

anhydrous CH_2Cl_2 solution.

SI 7. Transient decay spectra of *R*-ZnL in solution.

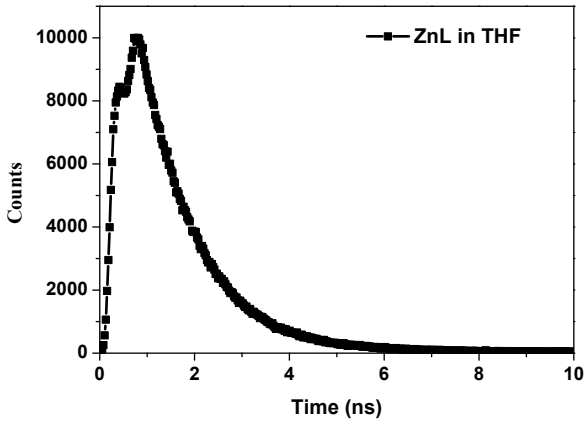

Figure S8. Transient decay spectra of *R*-ZnL, in solution of THF (1.0×10^{-4} mol·L^{-1}, λ_{ex} = 374 nm).

SI 8. EL color coordinates on the CIE 1931 chromaticity diagram of CP-OLEDs

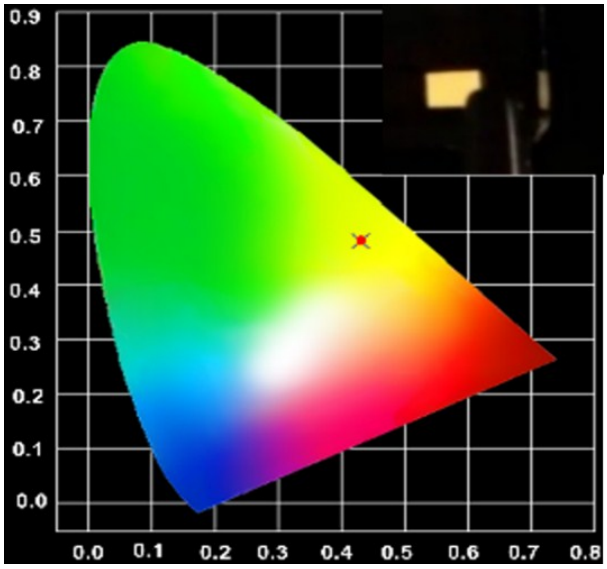

Figure S9. EL color coordinates on the CIE 1931 chromaticity diagram of CP-OLEDs

SI 9 Current density-voltage characteristics of the hole- and electron-only devices.

The carrier transporting ability of the Zn(II) complex were evaluated by single-carrier devices. The hole-only device adopted the structure of ITO/TAPC (45 nm)/*S*-ZnL (45 nm)/TAPC (45 nm)/Ag (100 nm), where TAPC at the anode and cathode was used to transport holes and prevent electrons, respectively. The structure of electron-only device was ITO/TmPyPb (45 nm)/*S*-ZnL (45 nm)/ TmPyPb (45 nm)/Ca (10 nm)/Ag (100 nm), in which TmPyPb at the anode and cathode was used to prevent hole injection and to facilitate electron transport, respectively. The current density-voltage characteristics of the hole- and electron-only devices are presented in **Figure S10**.

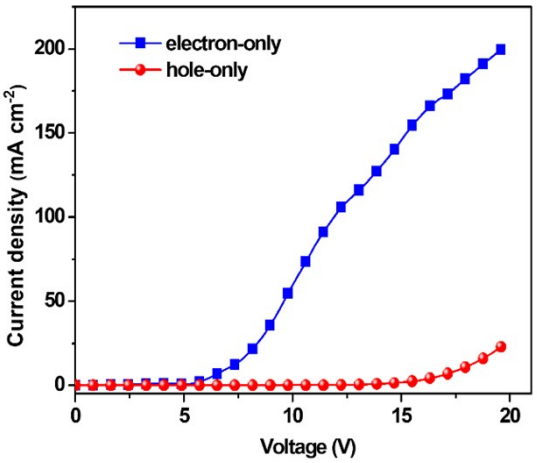

Figure S10. Current density-voltage characteristics of the hole- and electron-only devices.

SI 11. External quantum efficiency (EQE) of the devices of D and E

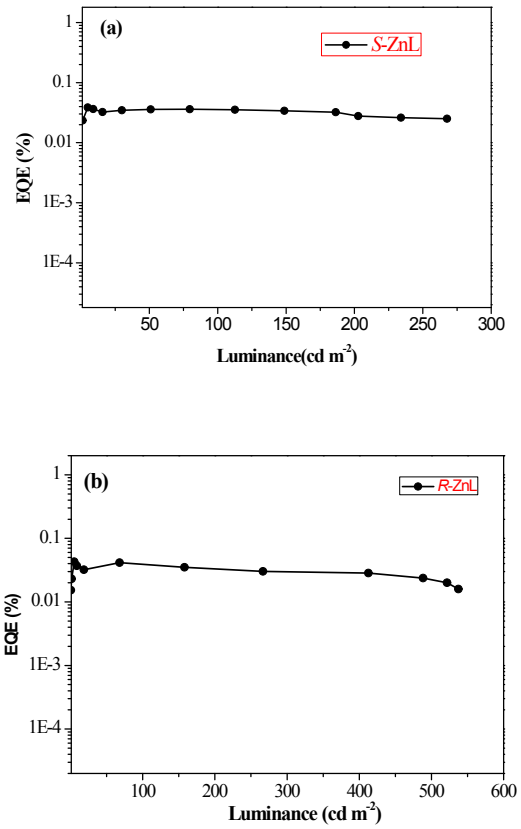

Figure S11. External quantum efficiency (EQE) of devices D (a) and E (b)